

LOAD TESTS ON 2-SPAN REINFORCED CONCRETE BEAMS STRENGTHENED WITH FIBRE REINFORCED POLYMER

Lander Vasseur¹, Stijn Matthys², Luc Taerwe³

*Department of Structural Engineering, Ghent University, Magnel Laboratory for Concrete Research
Technologiepark-Zwijnaarde 904, B-9052, Belgium*

Abstract: The structural behaviour of reinforced concrete beams strengthened in flexure with externally bonded FRP (Fibre Reinforced Polymer) reinforcement has been extensively investigated with respect to isostatic beams. However, limited information is available on the behaviour of continuous beams, strengthened with composite reinforcement. For flexural strengthening of a continuous beam the FRP can be applied above the middle support, at the two spans or at both locations. Through an analytical study and three full-scale experimental tests on reinforced concrete beams, with two spans of 5 m, the non-linear behaviour of strengthened continuous beams is investigated. It is verified in which degree moment redistribution is still present when applying this strengthening technique. Further, the different debonding mechanisms applicable to bonded FRP reinforcement are studied from the perspective of continuous beams. Because continuous beams typically have a moment line with different signs, most of the FRP laminate ends can be anchored in the compression zone. As a result, some debonding mechanisms, e.g. concrete rip-off and debonding at the anchorage zone can be avoided.

Keywords: *continuous concrete beam, flexural strengthening, FRP (Fibre Reinforced Polymer), EBR (Externally Bonded Reinforcement), non-linear behaviour, moment redistribution, debonding*

1 Introduction

Structures may need to be strengthened for different reasons, among which a change in function, implementation of additional services or to repair damage. Different strengthening techniques exist. Often applied is externally bonded reinforcement (EBR), based on fibre reinforced polymer (FRP), the so-called FRP EBR.

FRP EBR can be applied for the strengthening of existing structures, enhancing the flexural and shear capacity or to strengthen by means of confinement. This paper discusses flexural strengthening of 2 span reinforced concrete beams. Here, CFRP (Carbon FRP) laminates can be glued on the soffit of the spans and/or on the top of the mid-support [1, 2]. The efficiency of the FRP EBR strengthening technique is often limited by the capability to transfer stresses in the bond interface. Hereby bond failure between the laminate and the concrete may occur.

Further, for unstrengthened continuous beams a moment redistribution can be observed especially after yielding of one of the critical cross-sections. As a consequence a plastic hinge will be formed. For

strengthened concrete beams, after reaching the yield moment, the FRP strengthened cross-section is still able to carry additional load and the formation of a plastic hinge will be restricted.

The aim of this study is to have a better insight in the behaviour of reinforced concrete structures strengthened in flexure in a multi-span situation.

2 Debonding mechanisms on continuous beams

2.1 Different debonding mechanisms

Bond failure in case of FRP EBR implies the loss of composite action between the concrete and the FRP reinforcement. This type of failure is often very sudden and brittle. According to Matthys [3] different bond failure aspects can be distinguished.

2.1.1 Crack bridging

The externally bonded FRP will need to bridge cracks. In regions with significant shear forces, shear or flexural cracks have a vertical (v) and a horizontal (w) displacement. The vertical displacement of the concrete causes tensile stress perpendicular to the FRP EBR, which initiates debonding of the laminate (Fig. 1).

¹ PhD Student, lander.vasseur@ugent.be

² Professor, stijn.matthys@ugent.be

³ Professor, luc.taerwe@ugent.be

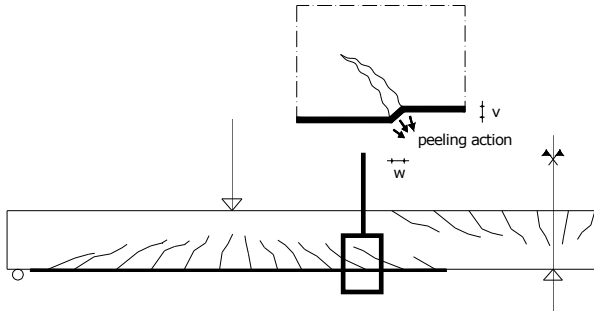


Figure 1: Peeling-off caused at shear cracks

2.1.2 Force transfer

The variation of tensile force in the FRP, due to the composite action between the FRP EBR and the concrete beam initiates bond shear stresses at the interface. The bond shear stress considered between two sections at a distance Δx equals:

$$\tau_b = \frac{\Delta N_{fd}}{b_f \Delta x} \quad (1)$$

These shear stresses have to be smaller than the bond strength between the concrete and the FRP reinforcement.

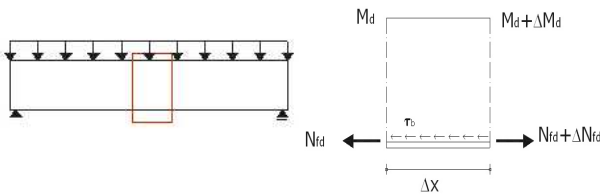


Figure 2: Peeling-off caused by force transfer

2.1.3 Curtailment and anchorage length

Theoretically the FRP reinforcement can be curtailed when the axial tensile force can be carried by the internal steel only. The remaining force in the FRP at this point needs to be anchored. The anchorage capacity of the interface is however limited, and hence the FRP may be extended to zones corresponding to low FRP tensile stresses.

2.1.4 Concrete rip-off

If a shear crack appears at the plate-end, this crack may propagate as a debonding failure at the level of the internal steel reinforcement. In this case the laminate as well as a thick layer of concrete will rip off.

Concrete rip-off also can occur due to a stress concentration at the laminate end.

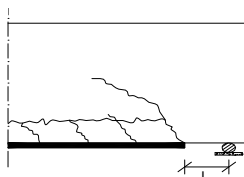


Figure 3: Concrete rip-off by plate end shear

2.2 Debonding mechanisms in continuous beams

To predict the debonding load, the available calculation models [4] are based on formulas which basically related to experiments on isostatic reinforced beam and pure shear bond tests.

The difference between isostatic beams and continuous beams, which is critical for these debonding mechanisms in continuous reinforced concrete beams, is the moment line with opposite signs. While the moment in the span is positive, the moment at the mid-support is negative. As a result, the compression zones in the spans are situated at the top of the beam, at the support the compression zone is situated at the soffit of the beam (shaded zones in Fig. 4). This allows in contrast to reinforced isostatic beams, to anchor the CFRP laminates in the compression zones (except for the end supports) (Fig. 5). By extending a laminate into these compression zones, two out of the four different debonding mechanisms will be avoided: debonding by a limited anchorage length and debonding by end shear failure (concrete rip-off).

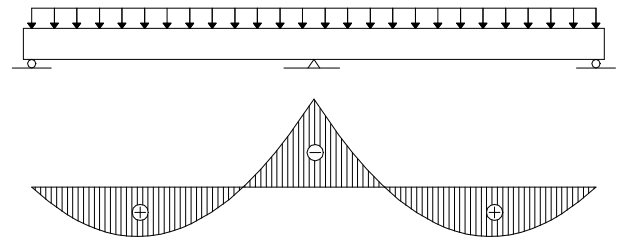


Figure 4: Moments with opposite signs in continuous beams



Figure 5: Anchoring laminates into compression zones

Debonding by limited anchorage length is prevented by extending the laminate into the compression zone because in this situation the tensile stress in the laminate is gradually reduced to zero, and anchored in a zone with small compressive stresses (no significant risk for buckling).

Debonding by end shear failure occurs at a shear crack at the end of the laminate. By extending the laminate into the compression zone, the plate-end reaches a zone where no shear cracks will be formed and neither concrete rip-off will appear.

Debonding mechanisms can be avoided by extending the laminate into the compression zone, hence beyond the point of contraflexure, which is the location where the internal moment equals zero. For calculating the exact location of this point, it has to be noticed that the point of contraflexure moves with increasing load, due to the non-linear moment redistribution.

3 Calculation model for continuous beams

3.1 Non-linear moment-curvature diagram

When performing a linear elastic analysis of a structure the following relationship between the moment and the curvature is used:

$$\frac{1}{r} = \frac{M}{EI} \quad (2)$$

where $1/r$ is the curvature, M the bending moment and $K = EI$ the bending stiffness. This stiffness is assumed to be constant and therefore independent of the value of the bending moment. However, for the cross-section of a concrete beam the moment-curvature diagram is non-linear. This non-linear character results in a variable bending stiffness, as shown in Fig. 6. Two cases are drawn in this graph, a cross-section with or without FRP. An important difference between these cases is the bending stiffness (slope of lines K_0 , K_1 and K_2). With FRP higher values for K are obtained than without FRP. This different behaviour will influence the moment redistribution of a continuous beam.

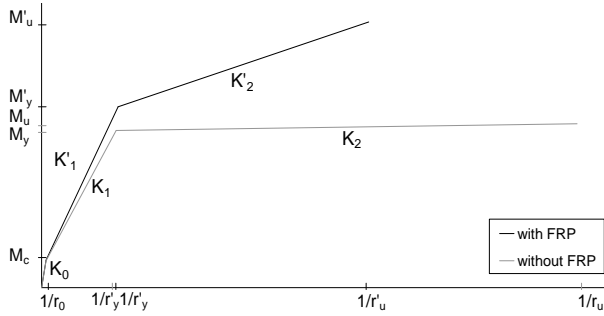


Figure 6: Moment-curvature diagram

If Fig. 6 is applied to a continuous beam, we start with the uncracked phase along the whole length of the beam, corresponding to the use of K_0 as bending stiffness. By increasing the load, the beam is characterized by cracked and uncracked zones, each with the related value of bending stiffness. This change of stiffness causes a first redistribution of moments. For the yield load F_y , one or more cross-sections reach the yield moment (M_y). In yield zones without FRP EBR, the bending stiffness K_2 is so small that plastic deformations appear in the critical cross-section and in a restricted area near to it. This is the formation of a so-called plastic hinge. The increasing load is mainly carried by the non plastic zones while the bending moment in the plastic hinge remains almost constant ($M_u \approx M_y$) or is slowly increasing. In zones with FRP EBR, the value of the bending stiffness is higher (K'_2). Also plastic deformations appear, but in a more limited way. The yielding zone still carries a significant part of the increasing load and the rotation of the plastic hinge is restricted.

3.2 General behaviour of continuous beams

Consider a continuous beam with two identical spans and symmetrical loaded by two point loads (Fig. 7). Focusing on one span, two zones can be defined, one zone with positive moments (above mid-support) and another with negative moments (in the spans). It is assumed that in each zone the bending stiffness is constant. So the mid-support zone and the span-zone have stiffness $K_{support}$ and K_{span} , respectively.

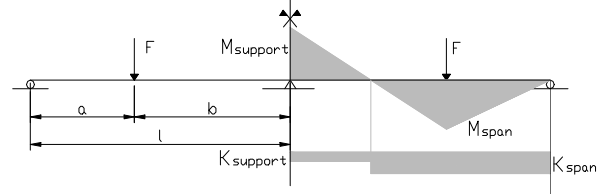


Figure 7: Continuous beam with variable bending stiffness (simplified to 2 stiffness zones)

Further, we define:

$$\lambda = \frac{a}{b} \quad m = \frac{M_{sup\ port}}{M_{span}} \quad k = \frac{K_{sup\ port}}{K_{span}} \quad (3)$$

By considering that the angle of rotation above the mid-support equals zero, the following equation can be obtained [5]:

$$(2 + 3\lambda)m^3 + (3 + 3\lambda - 2k\lambda^2)m^2 - k\lambda(3 + 4\lambda)m - (1 + \lambda)(1 + 2\lambda)k = 0 \quad (4)$$

With Eq. (4) the internal forces in the continuous beam can be calculated. In what follows, calculations are done for $a = 2$ m and $b = 3$ m. Hence with $\lambda = 2/3$ Eq. (4) changes into.

$$36m^3 + (45 - 8k)m^2 - 34km - 35k = 0 \quad (5)$$

This equation is shown in Fig. 8. For loads below the cracking moment, the mid-support zone and span zones are uncracked and the two zones nearly have the same bending stiffness. This condition correspond with $k = 1$. From Eq. (5) we obtain then $m = 0.9722 = m_{el}$. This value of m corresponds to the moment distribution following the classic theory of elasticity. Hereby, the relationship between acting load and internal moment is linear, as in the case of isostatic beams. By further increasing the load, the changing bending stiffnesses in different cross-sections modifies k thus the relation between the internal moments m . As a result the moment distribution deviates from the classic theory to the so-called non-linear moment-redistribution (see e.g. Fig. 10).

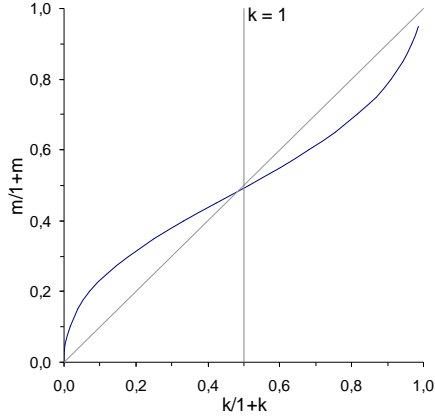


Figure 8: The relation of the moments m in function of the relation of the bending stiffnesses k

4 Experimental study

4.1 General overview of test program

4.1.1 Configuration

For the experimental study the test set-up of Fig. 7 is used. The total depth of the continuous concrete beam equals 400 mm and the width 200 mm. The continuous beam exists of two spans, each with a length of 5 m. The beam is loaded with one point load in each span. The locations of the point loads are at a distance of 3 meter of the mid-support and 2 meter from the end supports. Hence, a equals 2 m, b equals 3 m and $\lambda=2/3$ (referring to Eq. 3).

In the experimental program three full-scale continuous beams are tested with the same cross-section but different configurations of the internal and external reinforcement. The reinforcement configuration is shown in Figs. 9, 13 and 18. Beam CB1 is reinforced with a small amount of internal reinforcement in the spans and a large amount at the support. To compensate the small amount at the spans, externally bonded reinforcement (EBR) is applied only in the spans. The next beam (CB2) has internal reinforcement based on the linear elastic theory. In this case almost the same amount of internal reinforcement is used in the spans as at the mid support. As external reinforcement, laminates are glued on top of the beam above the mid-support as well as at the soffit of the beam in the spans. Finally a third beam is tested (CB3) with a large amount of internal reinforcement in the spans and a small amount at the support. As external reinforcement, EBR is only applied at the top of the beam above the mid-support.

During the tests both manual and electronic measurements are done. Firstly strain gauges are glued on top of the laminates. Further, load cells are placed under each support, by which the moment redistribution can be calculated. Next, the deflection in the spans is measured continuously by the use of LVDT's. Finally the strain of the internal steel and the concrete, especially in the compression zones, is measured manually.

4.1.2 Moment distribution

The moment redistribution is illustrated in Figs. 10, 14 and 19. These graphs give the span moment M_{span} and the mid-support moment $M_{support}$ at the critical section (where the moment is maximum), in function of the acting point load F (see Fig. 7). In each graph four different curves concerning the moment distribution are observed. First there is the linear curve which is the moment distribution calculated following the classic theory. Hereby, the relationship between the acting load and the internal moment is linear. Following, there is a non-linear dashed curve. This curve illustrates the non-linear moment distribution of the unstrengthened beam calculated according to the above mentioned non-linear theory. In addition, there are two non-linear curves, which represent the calculated and experimental non-linear moment distribution.

Finally a dashed horizontal line is drawn in the graphs. This curve illustrates the calculated load value where debonding is expected (calculating based on [4]).

4.1.2 Overview of test results

Based on the graphs of the moment redistribution (Fig. 10, Fig 14 and Fig. 19), two important conclusions can be made. A first observation is the good correspondence between the predicted and the experimentally obtained moment redistribution. Secondly, there can be concluded that the obtained debonding failure load is somewhat lower than predicted. This is especially the case for beams CB2 and CB3, for which debonding of the top laminate occurred. This can also be noted from tables 1 and 2, which give an overview of the ultimate loads and the debonding mechanisms.

Table 1: Overview of ultimate loads

	$F_{collaps,calc}$ [kN]	$F_{collaps,exp}$ [kN]	Ratio [%]
CB 1	157	153	97.5
CB 2	197	172	87.3
CB 3	124	115	92.7

Table 2: Overview of debonding mechanisms

	Debonding mechanism
CB 1	By crack bridging of laminate at soffit
CB 2	By crack bridging of laminate at top
CB 3	By crack bridging of laminate at top

In Table 3, a comparison is made between the ultimate load of the tested beams and the calculated ultimate load of these beams if they would not have been strengthened. Whereas the failure aspect of the strengthened beams is characterized by debonding, the failure aspect of the unstrengthened beams (as obtained from the calculation model) is characterized by yielding of the steel followed by concrete crushing.

Table 3: Comparison between reinforced and unreinforced continuous beams

	$F_{\text{strengthened}}$ [kN]	$F_{\text{unstrengthened}}$ [kN]	Ratio
CB 1	157	122	1.29
CB 2	197	118	1.67
CB 3	124	102	1.22

4.2 Continuous beam 1 (CB1)

4.2.1 Configuration

The first beam tested has internal reinforcement as shown in Fig. 9. The beam has low internal reinforcement ratio in the spans ($\rho_{s,span} = 0.48\%$) and high concentration of reinforcement above the mid-support ($\rho_{s,support} = 1.29\%$). As external reinforcement, two CFRP laminates with a length of 3750 mm are applied in the spans. The section of the CFRP laminate is 100 mm x 1.2 mm ($\rho_{f,span} = 0.17\%$).

The characteristics of the materials are given in Tables 4 and 5. These values result from standard tensile and compression tests.

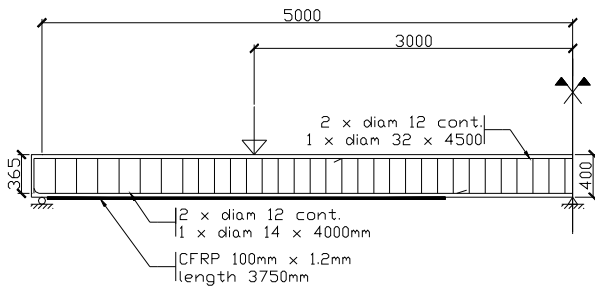


Figure 9: Internal steel configuration of CB1

Table 4: Properties of concrete and CFRP

	Concrete	CFRP
Compres. strength	38.0 N/mm ²	
Tensile strength	3.4 N/mm ²	2768 N/mm ²
Failure strain	0.35 %	1.46 %
E-modulus	35500 N/mm ²	189900 N/mm ²

Table 5: Properties of steel reinforcement

	Reinforcement in span	Reinforcement at support
Yielding strength	601 N/mm ²	530 N/mm ²
Yielding strain	0.28 %	0.25 %
Tensile strength	677 N/mm ²	701 N/mm ²
Failure strain	12.40 %	12.40 %
E-modulus	218000 N/mm ²	216000 N/mm ²

4.2.2 Moment redistribution

In Fig. 10, the moment redistribution of CB1 is illustrated as obtained from analytical calculation. For the unstrengthened beam, the formation of a plastic hinge can be noticed (vertical part of the dashed moment distribution curve). Whereas by the strengthened beam, although the strengthened spans still start to yield first, the FRP allows the spans to continue

resisting the additional load. At increasing load when the support starts to yield, a plastic hinge will be formed at this mid-support. Debonding of the FRP EBR is predicted following the fib code [4] at 157 kN.

Concerning the experimental data, a good agreement is observed with the calculated curve.

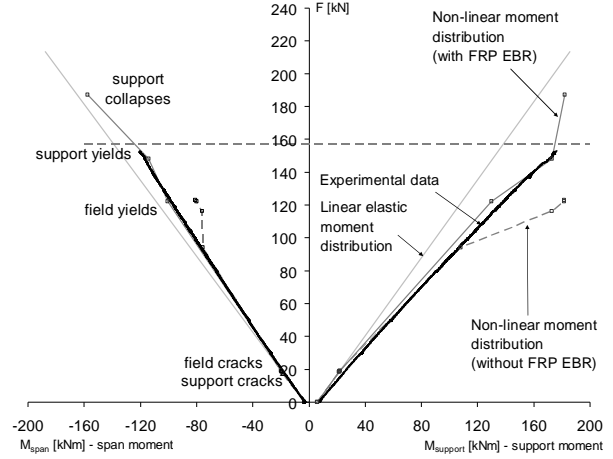


Figure 10: Moment redistribution of CB1

4.2.3 Debonding mechanism

The strengthened continuous beam fails by debonding of one of the CFRP laminates in the span. The appeared mechanism here is debonding by crack bridging. The debonding starts at a crack, located near the right point load, and debonds towards the mid support (Fig. 11). By testing the beam the laminate debonds at a load of 153 kN. This is 2.5% lower than the calculated value.

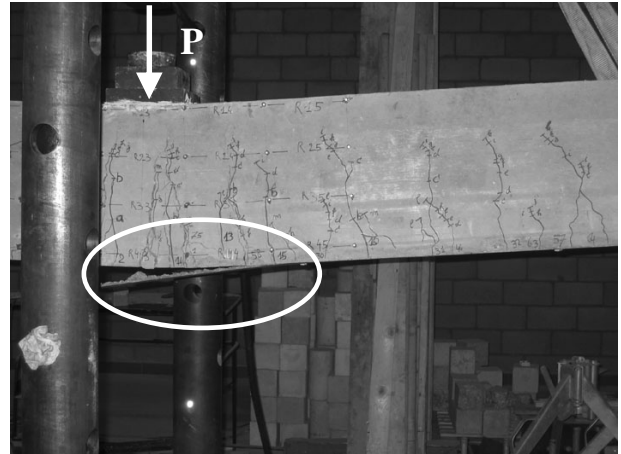


Figure 11: Debonding in the span by crack bridging

With its length of 3750 mm, the end of the laminate, near to the mid-support, extends about 500 mm in the compression zone. As mentioned above, this is done to avoid some debonding mechanisms. On the contrary the laminate has to resist to compressive strain in this zone. Fig. 12 gives a visual representation of the compression strains. As shown in the graph, the strain, measured by six strain gauges, has a linear character over the length of the laminate end. By visual inspection

of the laminate ends, anchored in the compression zones, during the test, no buckling of these laminate ends could be noticed.

In Fig. 12 a (small) shift of the point of contraflexure, caused by the non-linear moment redistribution can be observed.

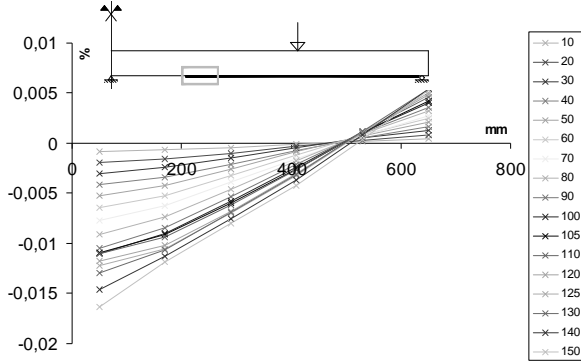


Figure 12: Strain in compression zone of laminate

4.3 Continuous beam 2 (CB2)

4.3.1 Configuration

The second tested continuous beam has internal reinforcement as shown in Fig. 13. The beam has an internal reinforcement ratio calculated according the linear elastic theory ($\rho_{s,span} = 0.68 \%$) and ($\rho_{s,support} = 0.61 \%$). As EBR, external reinforcement is used in the spans as well as at the mid support. Two CFRP laminates with a length of 3750 mm are applied in the spans ($\rho_{f,span} = 0.17 \%$), while one CFRP laminate with a length of 5000 mm is applied at the mid support ($\rho_{f,support} = 0.17 \%$). The section of the CFRP laminates is 100 mm x 1.2 mm.

The characteristics of the materials are given in Tables 6 and 7. These values result from standard tensile and compression tests

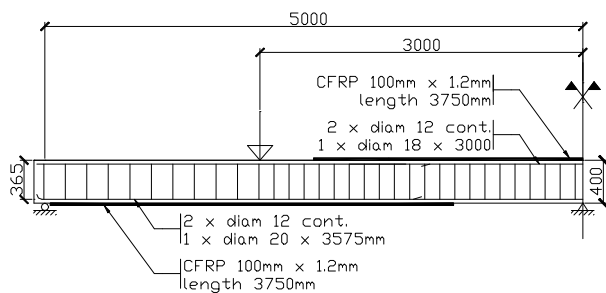


Figure 13: Internal steel configuration of CB2

Table 6: Properties of Concrete and CFRP

	Concrete	CFRP
Compres. strength	36.0 N/mm ²	
Tensile strength	3.3 N/mm ²	2768 N/mm ²
Failure strain	0.35 %	1.46 %
E-modulus	32000 N/mm ²	189900 N/mm ²

Table 7: Properties of steel reinforcement

	Reinforcement in span	Reinforcement at support
Yielding strength	570 N/mm ²	570 N/mm ²
Yielding strain	0.28 %	0.28 %
Tensile strength	670 N/mm ²	670 N/mm ²
Failure strain	12.40 %	12.40 %
E-modulus	210000 N/mm ²	210000 N/mm ²

*not tested, same values assumed as span

4.3.2 Moment redistribution

The moment redistribution of CB2 is illustrated in Fig. 14. Because the used amount of internal and external reinforcement is chosen nearly following the linear elastic moment distribution, hardly any moment redistribution is observed.

Following the non-linear theory, the support and the span yield at nearly the same moment, both in the strengthened and the unstrengthened beam. For the unstrengthened beam this results in a mechanism (formation of 3 plastic hinges at the same time). For the strengthened beam, due to the FRP EBR, the yielding sections are still able to carry additional load and at the same time plastic hinge formation is restricted.

Concerning the experimental data, a good agreement is observed with the calculated curve.

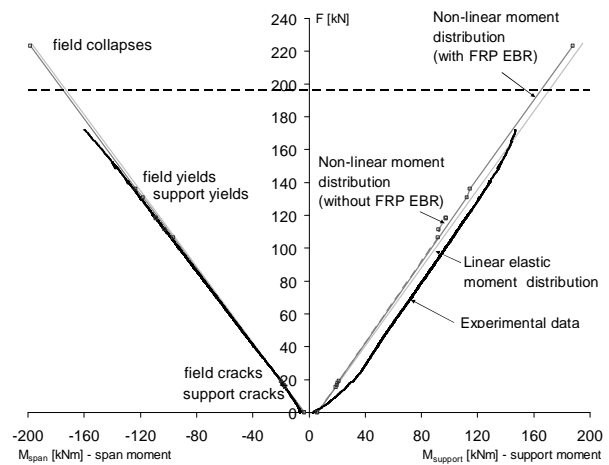


Figure 14: Moment redistribution of CB2

4.3.3 Debonding mechanism

In this case debonding occurs at the top laminate, above the mid support, by crack bridging (Fig. 15). Following the calculations, a debonding load of 197 kN is expected. Experimentally the laminate debonds at 172 kN. This is a difference of 25 kN or 12.7% of the calculated value following the fib code [4].

The debonding starts at a crack, located at the mid support, and debonds towards the left point load in Fig. 15.

The strain distribution at the FRP ends anchored in the compression zone is given in Figs. 16 and 17.



Figure 15: Debonding at the mid-support by crack bridging

As can be seen in Fig. 16, for the end of the soffit laminate near to the mid support, and in Fig. 17, for both ends of the top laminate, the strain caused by the compression is quasi linear over the length of the laminate end. In both cases the strain is measured by four strain gauges. By visual inspection of the laminate ends, anchored in the compression zones, during the test, no buckling of the laminate ends could be noticed.

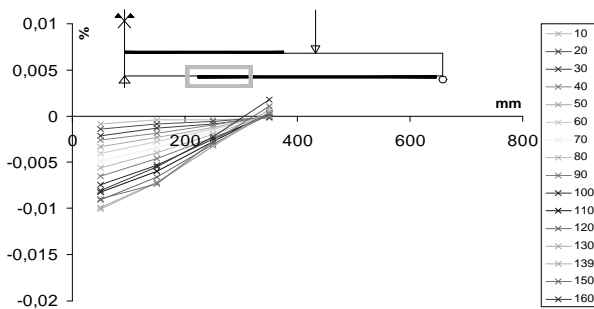


Figure 16: Strain in compression zone of soffit laminate

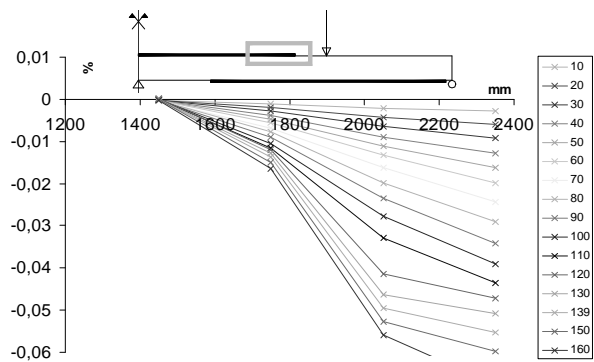


Figure 17: Strain in compression zone of top laminate

4.4 Continuous beam 3 (CB3)

4.4.1 Configuration

The last tested beam has internal reinforcement as shown in Fig. 18. The beam is designed with high internal reinforcement ratio in the spans ($\rho_{s,span} = 0.90\%$) and low amount of reinforcement above the mid-support ($\rho_{s,support} = 0.29\%$). As external reinforcement,

one CFRP laminate with the length of 5000 mm is applied at the mid support. The section of the CFRP laminate is 100 mm x 1.2 mm ($\rho_{f,support} = 0.17\%$).

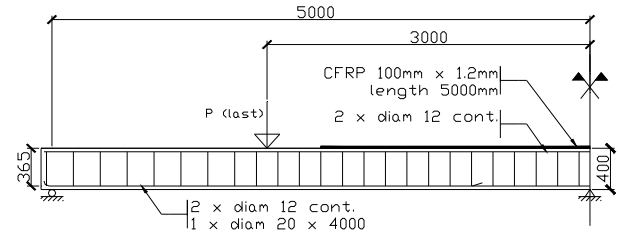


Figure 18: Internal steel configuration of CB3

The characteristics of the materials are given in Tables 8 and 9. These values result from standard tensile and compression tests.

Table 8: Properties of Concrete and CFRP

	Concrete	CFRP
Compres. strength	35.3 N/mm ²	
Tensile strength	3.2 N/mm ²	2768 N/mm ²
Failure strain	0.35 %	1.46 %
E-modulus	32000 N/mm ²	189900 N/mm ²

Table 9: Properties of steel reinforcement

	Reinforcement in span	Reinforcement at support
Yielding strength	589 N/mm ²	589 N/mm ²
Yielding strain	0.26 %	0.26 %
Tensile strength	674 N/mm ²	674 N/mm ²
Failure strain	12.40 %	12.40 %
E-modulus	22300 N/mm ²	223000 N/mm ²

*not tested, same values assumed as span

4.4.2 Moment redistribution

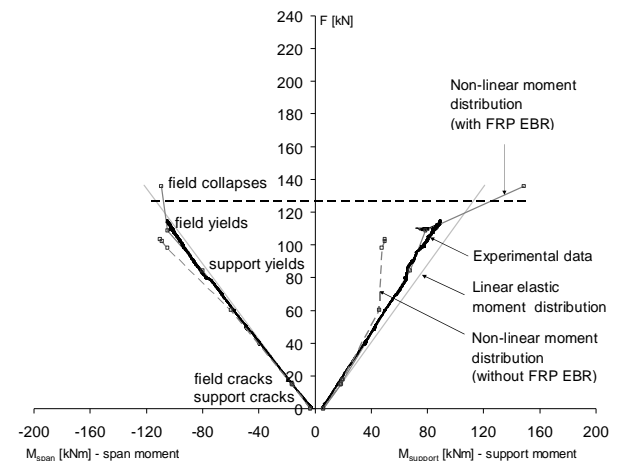


Figure 19: Moment redistribution of CB3

In Fig. 19, the moment redistribution of CB3 is illustrated. Following the non-linear theory, the mid support yields first. For the unstrengthened beam, after yielding of the mid support, a plastic hinge is formed (vertical part of the dashed moment distribution curve). For the strengthened beam, although the strengthened

mid support still start to yield first, the FRP allows the mid support to continue resisting the additional load. At increasing load when the spans start to yield, plastic hinges will be formed in the (unstrengthened) spans. The calculated debonding load following the fib code [4] is equal to 124 kN.

Concerning the experimental data, a good agreement is observed with the calculated curve.

4.4.3 Debonding mechanism

For this beam again debonding of the top laminate at the mid support occurs. Following the calculations, a debonding load of 124 kN is expected. Experimentally the laminate debonds at 115 kN. This is a difference of 9 kN or 7.3% of the calculated value.

The debonding starts at a crack, located at the mid support, and debonds towards the right point load in Fig. 20.

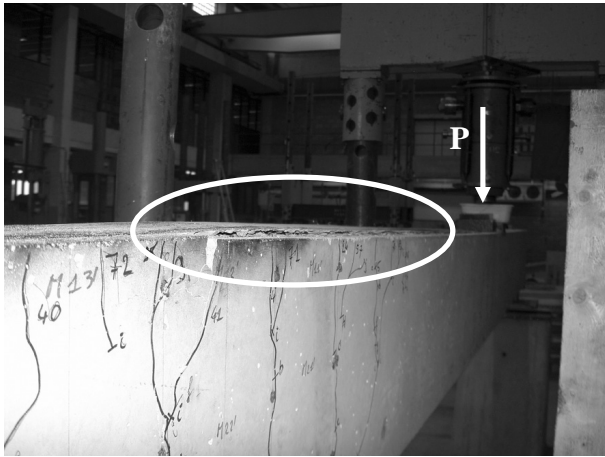


Figure 20: Debonding at the mid support by crack bridging

Fig. 21 gives the measured compression strains along the length of the laminate end, which is anchored in the compression zone. The measurements are carried out by the use of six strain gauges. As shown in the graph, the strain has a roughly linear character over the length of the laminate end. By visual inspection of the laminate ends, anchored in the compression zones, during the test, no buckling of the laminate ends could be noticed.

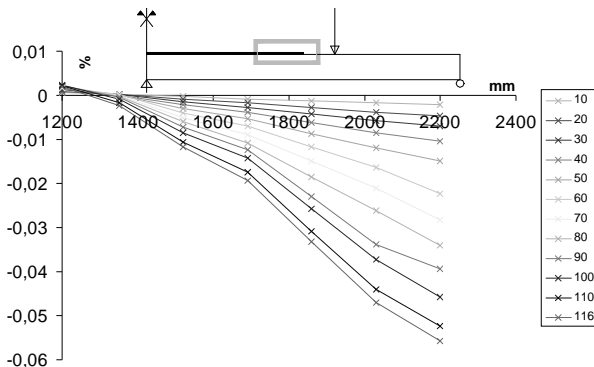


Figure 21: Strain in compression zone of top laminate

In Fig. 21 a (small) shift of the point of contraflexure caused by the non-linear moment redistribution can be observed.

5. Conclusions

For unstrengthened continuous beams a considerable moment redistribution can be observed, especially after plastic hinge formation. The latter occurs after reaching the yield moment in the critical cross-section (where the moment is maximum). Almost no moment redistribution is however observed if the yield moment is reached at the same time in both the spans and the mid-support.

In the case of FRP EBR strengthened continuous beams the observed behaviour largely depends on the amount of internal steel reinforcement in the span and mid-support and the strengthening configuration. After reaching the yield moment, the FRP strengthened cross-section is still able to contribute in carrying the additional load. Hence, such FRP strengthened cross-sections restrict the rotation of a plastic hinge at that location (and the related moment redistribution), but allow to transfer plastic hinge formation to unstrengthened cross-sections with high internal steel reinforcement ratio.

Acknowledgements

The authors acknowledge the financial support by FWO-Vlaanderen. The authors are grateful to ECC nv for providing and applying the CFRP laminates

References

- [1] El-Refaie, S.A., A.F. Ashour, and S.W. Garrity, *Sagging and Hogging Strengthening of Continuous Reinforced Concrete Beams Using Carbon Fiber-Reinforced polymer Sheets*. ACI Structural Journal, 2003. **Vol. 100**: p. 446-453.
- [2] Ashour, A.F., S.A. El-Refaie, and S.W. Garrity, *Flexural strengthening of RC continuous beams using CFRP laminates*. Cement and Concrete Composites, 2004. **26(7)**: p. 765-775.
- [3] Matthys, S., *Structural behaviour and design of concrete members strengthened with externally bonded FRP reinforcement*, in *Department of Structural Engineering*. 2000, Ghent University: Ghent. p. 345.
- [4] *fib bulletin 14, Externally bonded FRP reinforcement for RC structures*. 2001, International federation for structural concrete, Lausanne.
- [5] Taerwe, L. and B. Espion. *Serviceability and the Nonlinear Design of Concrete Structures*. in *IABSE PERIODICA 2/1989*. 1989.